



The Society shall not be responsible for statements or opinions advanced in papers or discussion at meetings of the Society or of its Divisions or Sections, or printed in its publications. Discussion is printed only if the paper is published in an ASME Journal. Authorization to photocopy for internal or personal use is granted to libraries and other users registered with the Copyright Clearance Center (CCC) provided \$3/article is paid to CCC, 222 Rosewood Dr., Danvers, MA 01923. Requests for special permission or bulk reproduction should be addressed to the ASME Technical Publishing Department.

Copyright © 1999 by ASME

All Rights Reserved

Printed in U.S.A.

## SYSTEMATIC REDUCTION OF STRESS LEVELS FOR A THERMALLY HIGH LOADED CERAMIC NOZZLE VANE WITH TRAILING EDGE EJECTION

M. Dilzer, A. Schulz, S. Wittig



Lehrstuhl und Institut für Thermische Strömungsmaschinen  
Universität Karlsruhe (T.H.)  
Karlsruhe (Germany)

### ABSTRACT

This paper presents a design concept for thermally high loaded ceramic shell components, that is developed at the Institute for Thermal Turbomachinery (ITS, University of Karlsruhe). The aim is to obtain homogenous temperature distribution in the ceramic structure for the whole operating cycle of the engine.

Based on simple flat wall considerations design guidelines are introduced to reduce the dominant thermally induced stresses in ceramic components. The concept includes a systematic adjustment of the local cooling configuration and the local wall thicknesses according to the local thermal boundary conditions.

The concept is applied to increase the reliability of a directly cooled Sintered Silicon Carbide first stage nozzle vane with trailing edge ejection for a 70MW stationary gas turbine. Finite element analyses demonstrate that the application of this methodology leads to a rather uniform temperature distribution in the ceramic structure and therefore to low stress levels for steady state and for tripping conditions.

A transformation of the theoretically derived optimum cooling configuration to a technically feasible cooling setup is performed in the purpose of real engine application. It is found that some differences between optimum and technically feasible cooling configuration (mainly located at the trailing edge region) are of minor importance. The results of failure probability calculations (ITS fracture statistics code CERITS) confirm significantly improved reliability of the ceramic nozzle vane.

### NOMENCLATURE

|                    | Symbols                      |                       |
|--------------------|------------------------------|-----------------------|
| T                  | Temperature                  | [K]                   |
| $\bar{T}$          | Mean Temperature             | [K]                   |
| t                  | Time                         | [s]                   |
| s                  | Width of the Ejection Slot   | [m]                   |
| d                  | Wall Thickness               | [m]                   |
| x                  | Surface Distance             | [m]                   |
| $x_{rel}$          | Relative Surface Distance    | [%]                   |
| q                  | Specif. Heat Flux            | [W/m <sup>2</sup> ]   |
| $c_p$              | Heat Capacity                | [J/kgK]               |
| Const <sub>1</sub> | Hot Gas Temperature Gradient | [K/s]                 |
| Const <sub>2</sub> | Heat Transfer Gradient       | [W/m <sup>2</sup> Ks] |
|                    |                              | ]                     |
| h                  | Heat transfer Coefficient    | [W/m <sup>2</sup> K]  |
| $\lambda$          | Thermal Conductivity         | [W/mK]                |
| $\rho$             | Density                      | [kg/m <sup>3</sup> ]  |

### Subscripts

|       |                                    |
|-------|------------------------------------|
| HG    | Hot Gas                            |
| CG    | Cooling Gas                        |
| Cer   | Ceramic                            |
| stat. | Stationary                         |
| opt.  | Optimum Cooling Conf.              |
| tec.  | Technically Feasible Cooling Conf. |

### INTRODUCTION

Present stationary gas turbine engines operate at turbine inlet temperatures that exceed the maximum allowable wall temperatures of the applied superalloys by far. This requires extensive cooling of the metallic components in the hot gas path.

The amount of cooling air is considerable and reduces the benefits in thermal efficiency, that are intended by increasing the turbine inlet temperature. The replacement of metallic components by relatively low-cooled ceramic parts with superior high temperature properties has substantial potential to improve the total thermal efficiency of the operating cycle. SiC is considered to be the most promising material for operating temperatures up to 1673K since it shows no significant drop in strength with increased temperatures [1].

Promising approaches to introduce ceramic components into gas turbines were carried out through development of a convectively cooled multi-layered hybrid design [2,3]. The intention was to obtain homogenous temperature distributions in the ceramic structure, i.e. the structure is low cooled and has temperatures close to the hot gas temperature. Further increases in turbine inlet temperatures, which are still desired, would lead to material temperatures that exceed the limited oxidation stability of the material considered (1673K, SiC). Particularly in the trailing edge region problems will arise due to the constraints in the cooling capabilities.

To overcome the problems indicated, the development of a directly cooled first stage ceramic nozzle vane with trailing edge ejection has gained special interest [4]. But so far, there has been no systematic approach to obtain reliable components. The requirement of meeting the high standards of reliability in gas turbine applications makes it necessary to setup design guidelines in order to reduce the dominant thermally induced stresses.

For this reason it is essential to analyze the thermal behavior of ceramic structures under typical gas turbine operating conditions, for steady state and for transient thermal boundary conditions.

This paper presents a simple flat wall heat transfer model for ceramic shell elements and the transformation of the achieved results to systematic design methodologies for ceramic components in the hot gas section of gas turbines. The goals (homogeneous temperatures and low thermal stresses respectively) are verified by finite element analyses of a first stage ceramic nozzle vane for a 70MW stationary gas turbine. Finally the results are evaluated by failure probability calculations taking into account fast fracture mode calculations for tripping conditions and slow-crack-growing effects for continuous operation [5].

## GEOMETRY AND BOUNDARY CONDITIONS

The specifications for the exemplary engine considered and the first stage stator are shown in Table 1. The outline form of the vane profile is changed slightly in order to

account for the demands arising from the application of ceramic materials. Without affecting the aerodynamics strongly the cooling capabilities are improved significantly by increasing the thickness of the trailing edge region.

Table 1: Specifications for the Engine and the First Stage Stator

|                    |                           |   |
|--------------------|---------------------------|---|
| Engine             | Rating                    | 70 MW   |
|                    | Pressure Ratio            | 17  |
|                    | Turbine Inlet Temperature | 1673 K  |
| First Stage Stator | Design                    | Directly Cooled/<br>Trailing Edge Ejection<br>Untwisted Airfoil<br>Integrated Sidewalls |
|                    | Material                  | Sintered Silicon Carbide  |
|                    | Vane Height               | 58 mm   |
|                    | Chord Length              | 60 mm   |

The local boundary conditions on the hot gas side are calculated using the ITS boundary layer code ALFA [6]. The external heat transfer coefficient  $h_{HG}$  varies between approx. 1700 and 6000 W/m<sup>2</sup>K. The gas path flow temperature varies with the radial position due to the specific combustor outlet conditions [2].

Transient boundary conditions are considered for the complete operating cycle of a gas turbine engine (including tripping conditions) [7].

## DESIGN OPTIMIZATION

Despite having excellent high temperature properties, the application of ceramic components in the hot gas section of gas turbine engines is rather difficult since these materials are very brittle and are unable to reduce stresses by plastic deformation. The introduction of these materials requires design principles that are taking into account these unfavorable properties.

The dominant stresses in ceramic vane profiles are induced by temperature gradients in the ceramic component [2,3,4]. The reliability of ceramic parts can be improved in reducing the thermal stresses for continuous operation and for transients as well.

The flat wall model of the ceramic shell component is given in Figure 1. Concentrating on steady state conditions the local heat flux can be described as :

$$\dot{q} = \frac{T_{HG} - T_{CG}}{\frac{1}{h_{HG}} + \frac{1}{h_{CG}} + \frac{d_{Cer}}{\lambda_{Cer}}} \quad (1)$$

or as:

$$q = \frac{T_{HG} - \bar{T}_{Cer}}{\frac{1}{h_{HG}} + \frac{d_{Cer}}{2\lambda_{Cer}}} \quad (2)$$

The local thermal boundary conditions are fixed due to the local hot gas flow ( $h_{HG}, T_{HG}$ ) and the local cooling gas Temperature ( $T_{CG}$ ) respectively. Furthermore the thermal conductivity  $\lambda_{Cer}$  is a fixed material constant and can not be included to adjust the thermal behavior of the ceramic structure. For steady state considerations as performed in this section the thickness of the ceramic shell  $d_{Cer}$  is assumed to be constant for the whole structure.

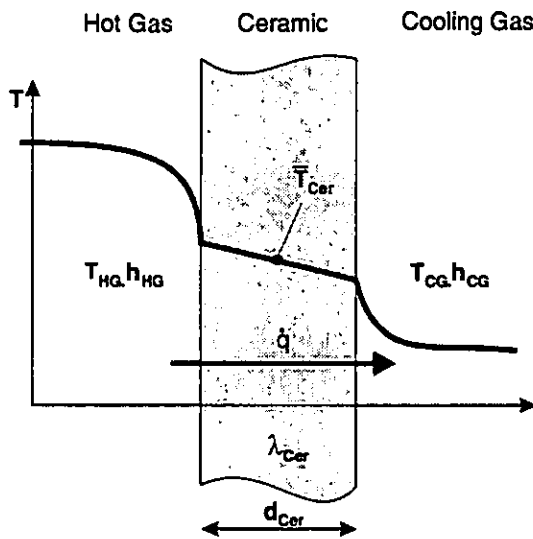


Figure 1: Flat Wall Model of the Ceramic Shell (Steady State Conditions)

The mean temperature  $\bar{T}_{Cer}$  ought to be constant to reduce thermally induced stresses. The remaining free parameter to adjust the local wall heat flux is the local heat transfer coefficient  $h_{CG}$  on the cooling gas side. Uniform temperature distribution is achieved by adjusting the local cooling configuration according to the given local thermal boundary conditions on the hot gas side:

$$h_{CG} = \frac{h_{HG}(\bar{T}_{Cer} - T_{HG})}{\frac{1}{2\lambda_{Cer}} d_{Cer} h_{HG} (T_{HG} + T_{CG} - 2\bar{T}_{Cer}) + T_{CG} - \bar{T}_{Cer}} \quad (3)$$

Figure 2 shows an exemplary distribution for the local heat transfer coefficient on the cooling gas side  $h_{CG}$  as a

function of the local heat transfer coefficient on the hot gas side  $h_{HG}$  and the local cooling gas temperature  $T_{CG}$ . The other parameters are fixed to typical values. The optimum heat transfer coefficient on the cooling gas side  $h_{CG}$  slightly increases with increased cooling gas temperatures  $T_{CG}$  and significantly increases with increased heat transfer coefficients on the hot gas side  $h_{HG}$ .

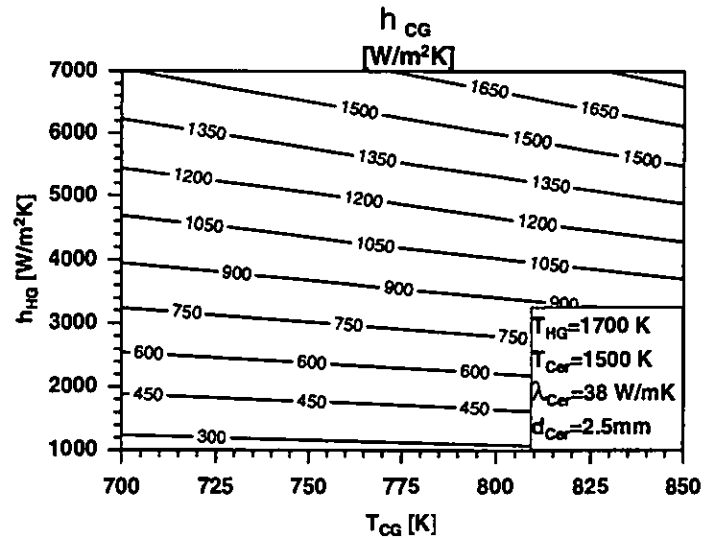


Figure 2: Adjustment of the Local Cooling Configuration:  $h_{CG} = f(h_{HG}, T_{CG})$

As mentioned before it is important to maintain this homogenous temperature distribution for the whole operating cycle of the engine. For this reason the flat wall model of the ceramic shell component is changed to allow for transient thermal boundary conditions (Figure 3)

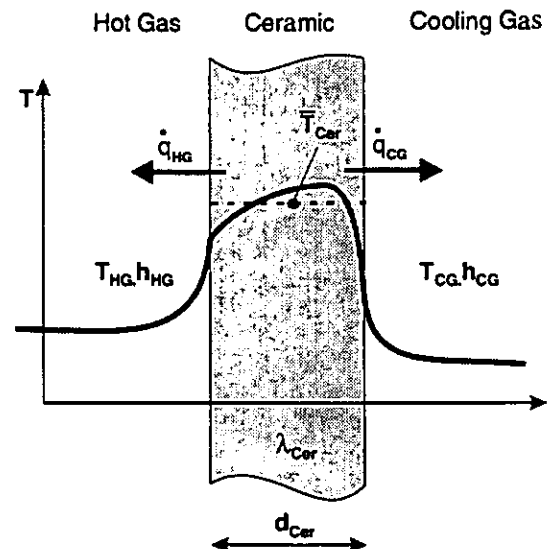


Figure 3: Flat Wall Model of the Ceramic Shell (Transient Conditions)

Some assumptions are made in order to simplify the heat transfer problem:

- Neglecting of temperature gradients normal to the wall surface. (This can be permitted since the conductive heat transfer rate exceeds the convective heat transfer rate by far (Biot Number  $\gg 1$ ):

$$T_{Cer, HG} = T_{Cer, CG} = \bar{T}_{Cer} \quad (4)$$

- The temperature and the heat transfer coefficient on the hot gas side vary linearly with the time for the first few seconds after the fuel-cutoff:

$$T_{HG}(t) = T_{HG, stat} - CONST_1 * t \quad (t <<) \quad (5)$$

$$h_{HG}(t) = h_{HG, stat} - CONST_2 * t \quad (t <<) \quad (6)$$

- The thermal boundary conditions on the cooling gas side do not vary within the first few second after the fuel-cutoff:

$$T_{CG}(t) = T_{CG, stat} \quad (t <<) \quad (7)$$

$$h_{CG}(t) = h_{CG, stat} \quad (t <<) \quad (8)$$

Taking these assumptions into account the wall heat fluxes can be described as:

$$\dot{q}_{HG}(t) = h_{HG}(t)(T_{HG}(t) - \bar{T}_{Cer}(t)) \quad (9)$$

$$\dot{q}_{CG}(t) = h_{CG}(T_{CG} - \bar{T}_{Cer}(t)) \quad (10)$$

A verification of this approximations is performed comparing the temperature gradients induced during tripping conditions. Figure 4 shows the mean wall temperatures  $\bar{T}_{Cer}(t)$  resulting from analytical calculations taking into account all assumptions listed above and the results of a finite element analysis for the flat wall model. The comparison shows that there are small differences, which clearly supports the validity of the assumptions.

The local heat balance for the ceramic shell can be formed as follows:

$$\dot{q}_{HG}(t) + \dot{q}_{CG}(t) = d_{Cer} \rho_{Cer} c_{P, Cer} \frac{\partial}{\partial t} \bar{T}_{Cer}(t) \quad (11)$$

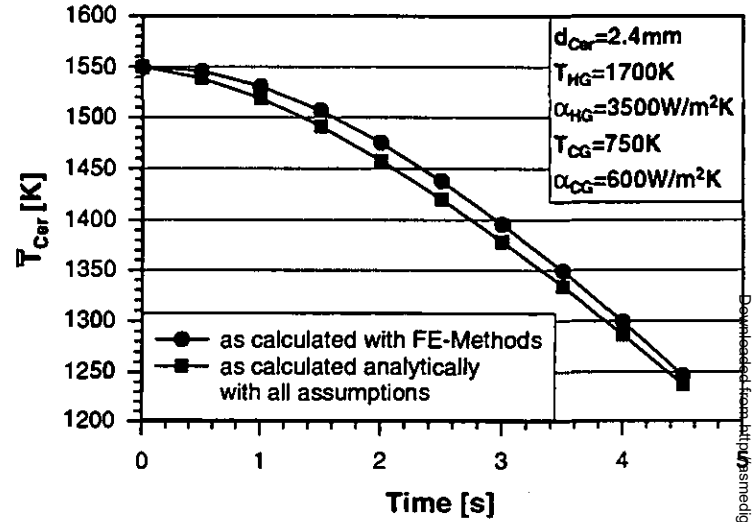


Figure 4: Comparison of Calculated Temperature Gradients (Tripping Conditions)

The mean wall temperature of the ceramic component at the begin of the fuel-cutoff is assumed to be constant due to the optimization for continuous operation. Therefore, the temperature distribution can be kept homogenous if the temperature gradients  $\delta/\delta t \bar{T}_{Cer}(t)$  are forced to be constant for the whole ceramic component. Taking Equation 11 the local temperature gradients can be adjusted by carefully varying the local wall thicknesses  $d_{Cer}$ , which is known to be a powerful approach to reduce temperature gradients during transient operation [2,3,8]:

$$\frac{\partial}{\partial t} \bar{T}_{Cer}(t) = \frac{\dot{q}_{HG}(t) + \dot{q}_{CG}(t)}{d_{Cer} \rho_{Cer} c_{P, Cer}} \quad (12)$$

For a given temperature gradient  $\delta/\delta t \bar{T}_{Cer}(t)$  the local wall thicknesses  $d_{Cer}$  have to be chosen according to the following equation:

$$d_{Cer} = \frac{h_{HG}(t)(T_{HG}(t) - \bar{T}_{Cer}(t)) + h_{CG}((T_{CG} - \bar{T}_{Cer}(t)))}{\rho_{Cer} c_{P, Cer} \frac{\partial}{\partial t} \bar{T}_{Cer}(t)} \quad (13)$$

This differential equation is not be solved for different instants in time since  $d_{Cer}$  can not be a function of time. To overcome this problem the optimum thickness of the ceramic shell is adjusted for thermal boundary conditions occurring 2.5 seconds after fuel-cutoff which is found to lead to the most favorable results. The optimum thicknesses of the ceramic shell structure  $d_{Cer}$  that are obtained for this approach are given in Figure 5. It has to be noted that this variation of the wall thicknesses

is restricted on fabrication aspects and on the function (here: aerodynamic aspects) of the component.

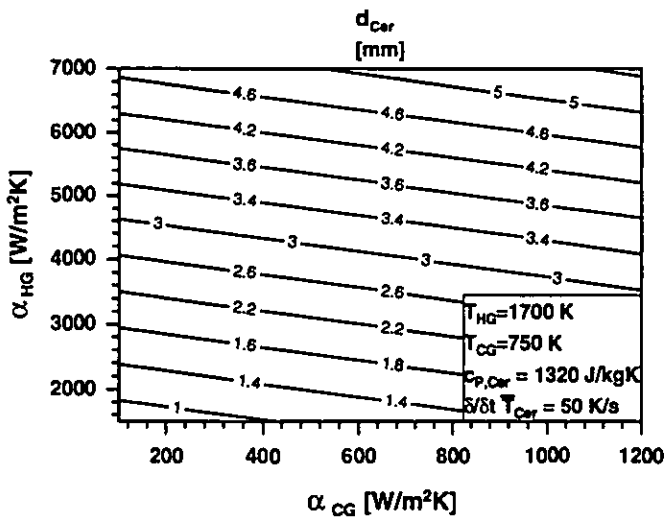


Figure 5: Adjustment of the Local Wall Thickness:  $d_{Cer} = f(h_{HG}, h_{CG}, t=2.5s)$

The optimum wall thickness  $d_{cer}$  increases strongly with increased heat transfer coefficients on the hot gas side  $h_{HG}$  and increases slightly with increased heat transfer coefficients on the cooling gas side  $h_{CG}$ .

### THERMALLY OPTIMIZED NOZZLE VANE

The finite element model of the nozzle vane is generated according to the design guidelines which were set up above (Figure 6). The wall thickness  $d_{Cer}$  of the vane profile varies from 2.17mm to 3.65mm at the stagnation point area where the heat transfer coefficients on the hot gas side changes strongly. The local wall thicknesses in the trailing edge region is excluded from the adjustment due to the given outline form and the given width  $s$  of the slot for the trailing edge ejection. The width of the continuous slot is specified to  $s=0.5mm$  which is found to guarantee reasonable heat transfer coefficients on the cooling gas side without reducing the local wall thicknesses considerably.

The thermal boundary conditions on the hot gas side and the systematic adjustment of the local cooling configuration is implemented to the computational model.

Finite element analyses are carried out considering the whole operating cycle of the engine (ignition – continuous operation – scheduled shutdown – fuel-cutoff). The resulting maximum and minimum temperatures and principal stresses in the ceramic shell are shown in Figure 7.

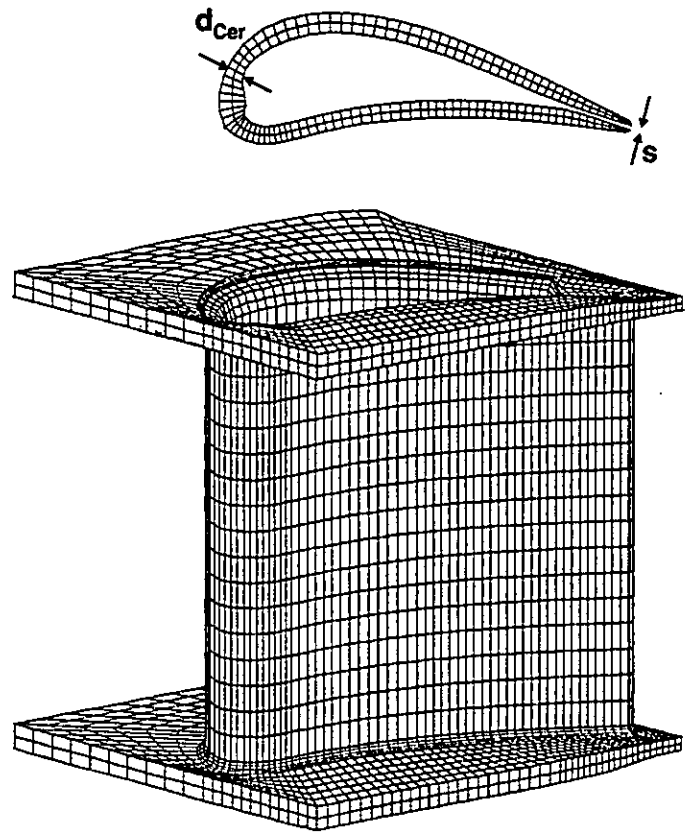


Figure 6: Finite Element Model of the Optimized Nozzle Vane

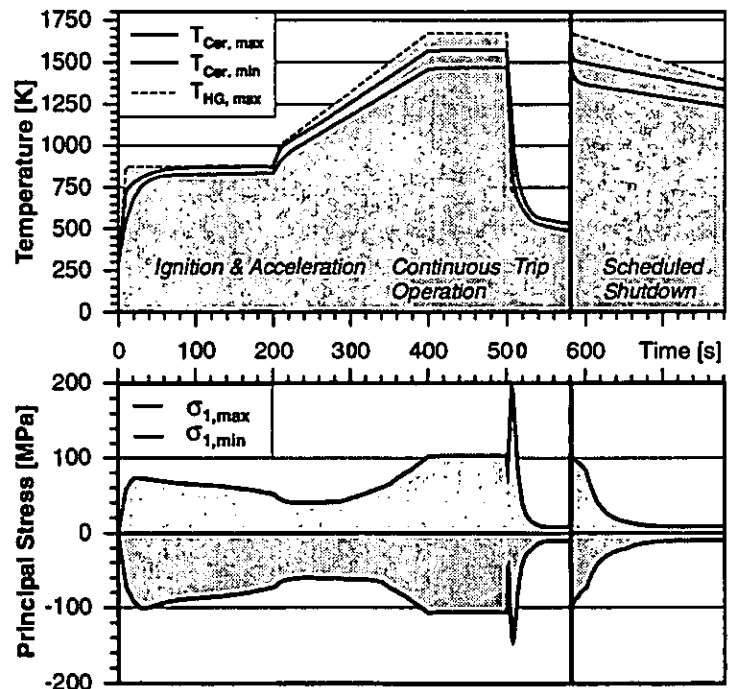


Figure 7: Max. and Min. Temperatures and Principal Stresses (Optimum Cooling Configuration)

It becomes obvious that there is only a small difference between the minimum and maximum temperatures for the whole operating cycle of the engine. The maximum stresses remain below 100 MPa and 180 MPa for continuous operation and for tripping conditions respectively. If compared with other efforts this is a significant reduction of the stress level. For continuous operation the induced stresses do not exceed 40% of the maximums that have been calculated by Day et al.(1998) and Tsuchiya et al.(1995) for Silicon Nitride vanes [4,9].

A transformation of the theoretically derived cooling configuration to a technically feasible cooling setup is performed. Therefore the vane profile is divided into 3 areas with different cooling methods (Figure 8):

- ① Impingement cooled stagnation point area
- ② Slightly convectively cooled mid-chord section
- ③ Trailing edge ejection

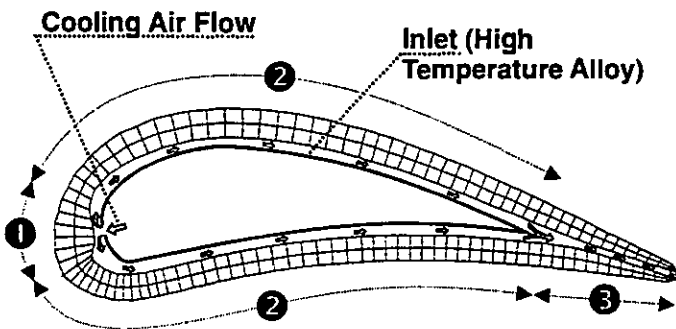


Figure 8: Cooling Setup

The calculation of the local heat transfer coefficients is carried out using correlations for impingement cooled convex surfaces [10] and correlations for flows through two-dimensional channels.

An inlet (high temperature alloy) is placed inside the ceramic shell structure. This inlet is supplied with cooling air, which is ejected through a continuous slot on the thermally high loaded stagnation point area ①. Cooling air then passes through the gap between the ceramic shell and the inlet ②. A variation of the local width of this gap makes it possible to adjust the local heat transfer coefficients  $\alpha_{CG}$ . This configuration allows the cooling air flow to heat up before entering the trailing edge ejection slot. Thus the local wall heat fluxes in the trailing edge region ③ are reduced, even though the narrow slot width results in high heat transfer coefficients. But for all that there is still a considerable discrepancy between optimum and technically feasible cooling configuration in the trailing edge region as shown in Figure 9 at vane mid-height. This difference arises from the simplification of the cooling setup. It is assumed that the total amount of

cooling air that is needed for the impingement cooled leading edge region is entirely ejected through the trailing edge slot, which leads to extremely high heat transfer coefficients in the slot.

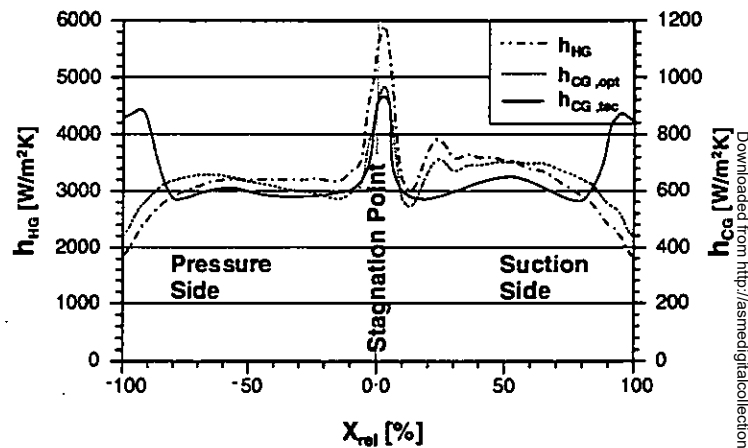


Figure 9: Heat Transfer Coeff. at Vane Mid-Height: Optimum ↔ Technically Feasible Config.

The results of the finite element analyses for the ceramic nozzle vane with a cooling configuration considering aspects of technical feasibility (Figure 10, right side) are compared to the results for the optimum cooling configuration (left side). At steady state conditions the maximum wall temperature is located at the stagnation point area and is not affected by the different heat transfer coefficients at the trailing edge region. For both configurations the temperature distribution is rather uniform in the whole ceramic structure which indicates the efficiency of the developed design principles. However, the minimum wall temperature at the trailing edge is about 40 K lower, if the technical feasible setup is compared to the optimum cooling setup.

The corresponding stress distributions for steady state conditions are shown at the bottom of Figure 10. Due to the different temperature distributions in the trailing edge region the maximum induced thermal stresses rise from approx. 100 MPa (optimum cooling setup) to approx. 170 MPa (technically feasible setup). These high stresses are concentrated on small areas while the rest of the ceramic structure is relatively low stressed. The maximum stresses are located at the cooling gas side of the stagnation point area and at the tip of the trailing edge for the optimum and the technically feasible cooling setup respectively.

Considering transient conditions taking place after fuel cutoff the chart on the left indicates that the different temperature distributions (i.e. the minimum wall temperatures) at the beginning of the trip, which are due to

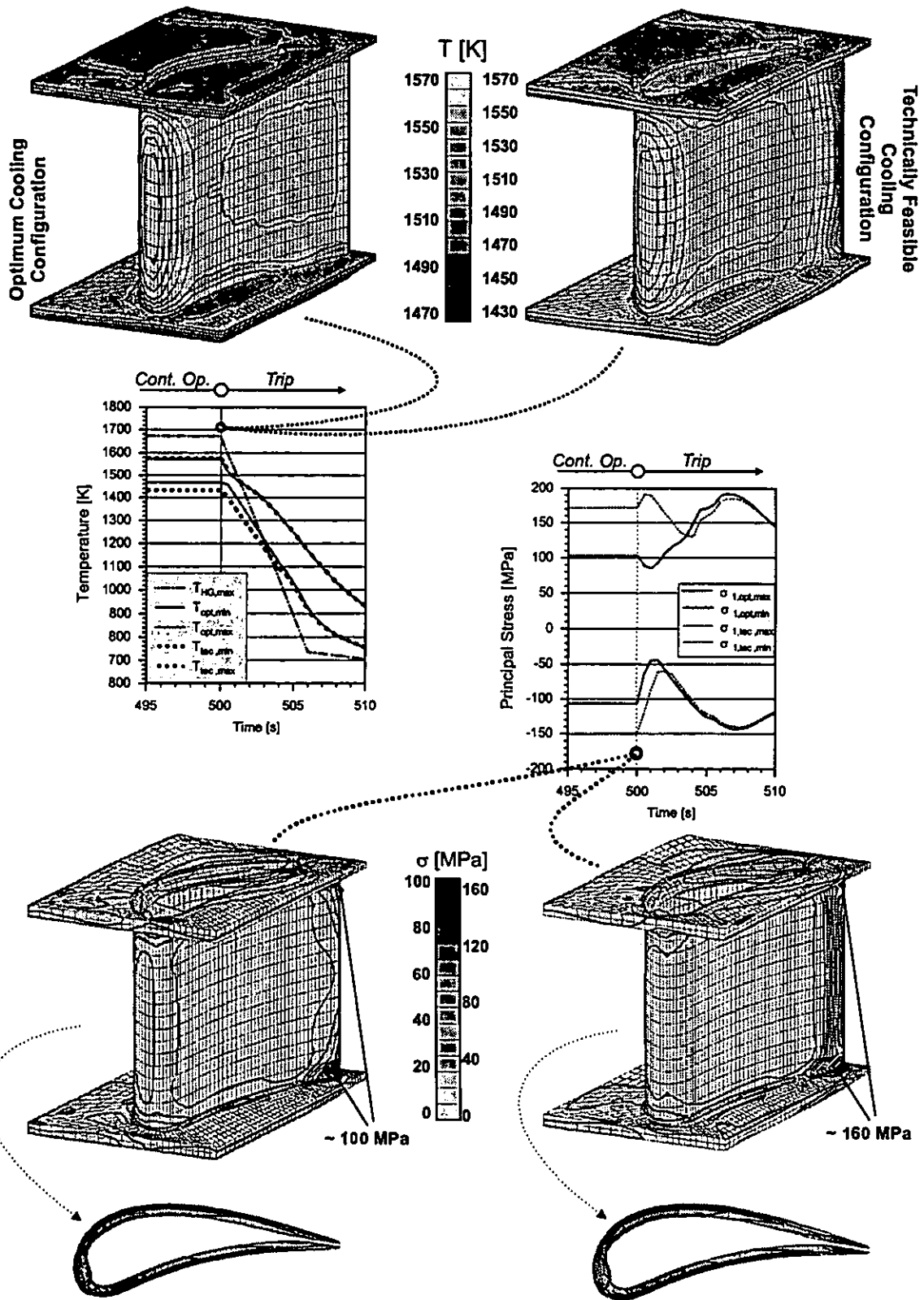


Figure 10: Comparison of Temperature and Stress Distributions:  
Optimum ↔ Technically Feasible Cooling Configuration

the different cooling configurations decrease with time.

The maximum induced stresses of about 190 MPa occur during tripping conditions for both configurations as shown in the chart on the right side of Figure 10. For the optimum cooling configuration the maximum stress occurs approx. 6 seconds after fuel cutoff. In contrast to this the technically feasible setup shows two stress peaks after 0.5 and 6 seconds respectively.

Failure probability calculations are carried out for steady state and for tripping conditions using the ITS Fracture Statistics Code CERITS (Table 2). Material properties for Norton NT-230 SSiC [1] are assumed.

Table 2: Failure Probability Calculations (ITS Fracture Statistics Code CERITS)

| Cooling Configuration | Mode                                 | Failure Probability [-] |
|-----------------------|--------------------------------------|-------------------------|
| Optimum               | 10000 h stat.<br>(Slow-Crack-Growth) | $1.5402 \cdot 10^{-7}$  |
|                       | Trip<br>Fast Fracture                | $6.2369 \cdot 10^{-7}$  |
| Technically Feasible  | 10000 h stat.<br>(Slow-Crack-Growth) | $6.9848 \cdot 10^{-5}$  |
|                       | Trip<br>Fast Fracture                | $9.6226 \cdot 10^{-7}$  |

As expected from the results of the stress analyses there is a considerable difference in failure probability when taking into account 10000 hours of continuous operation. Due to the relative low stress levels for the optimum cooling configuration the calculations result in failure probabilities of approx.  $1.5402 \cdot 10^{-7}$ . The technically feasible cooling setup with increased stresses for continuous operation causes failure probabilities of approx.  $6.9848 \cdot 10^{-5}$ .

Fast fracture mode calculations for the maximum stresses under tripping conditions (approx. 190 MPa for both configurations) reveal failure probabilities of  $6.2369 \cdot 10^{-7}$  and  $9.6226 \cdot 10^{-7}$  respectively.

These results prove sufficient probability of survival to guarantee reliable operation of the ceramic component and therefore, confirm the design principles developed.

## CONCLUSIONS

Design guidelines to reduce thermally induced stresses in ceramic shell components in the hot gas section of gas turbine engines are introduced. Based on a

simple flat wall heat transfer model the thermal behavior of the ceramic component is adjusted in order to achieve uniform temperature distribution in the whole structure for continuous and for transient operation of the engine.

The design principles, i.e. an adjustment of the local cooling configuration and the local wall thickness according to the local thermal boundary conditions, are applied to the first stage ceramic stator vane of a stationary gas turbine engine.

The optimized ceramic nozzle vane shows significantly reduced stress levels, as found by finite element analyses. A transformation of the optimized cooling configuration to a technically feasible cooling setup is performed.

Failure probability calculations (CERITS) demonstrate adequate reliability of the ceramic component for continuous operation and for tripping conditions as well.

The maximum wall temperatures remain below the oxidation limits of the SSiC-Material considered and, therefore offer potential for further increases in turbine inlet temperatures.

## ACKNOWLEDGEMENTS

The authors are grateful to the KKS (Keramikverbund Karlsruhe Stuttgart) which supported part of this work.

## REFERENCES

- [1] Hecht, N.L., Hongsang, R., Osborne, N.R., McCullum, D.E., Goodrich, S.M.: 'The thermal-Mechanical Behavior of Selected  $\text{Si}_3\text{N}_4$  and SiC Ceramics', ASME 96-GT-276, 1996
- [2] Gutmann, Ch., Schulz, A., Wittig, S.: 'A New Approach for a Low-Cooled Ceramic Nozzle Vane', ASME 96-GT-232, 1996
- [3] Dilzer, M., Gutmann, Ch., Schulz, A., Wittig, S.: 'Testing of a Low-Cooled Ceramic Nozzle Vane under Transient Conditions', ASME 98-GT-116, 1998
- [4] Day, W., Kouris, K., Holowczak, J., Blair, M., Hale, S., Bornemisza, T.: 'Development of Cooled, Ceramic First Stage Vanes for the FT8 Aero-derivative Gas Turbine', ASME 98-GT-133
- [5] Stürmer, G., Schulz, A., Wittig, S.: 'Life Time Prediction for Ceramic Gas Turbine Components', ASME 91-GT-96, 1991



[6] Sieger, K., Schiele, R., Kaufmann, F., Wittig, S., Rodi, W.: 'A Two-Layer Turbulence Model for the Calculation of Transitional Boundary-Layers', ERCOFTAC Bulletin (24), 1995

[7] Maghon H., Deblon, B., Schulenberg, T.: 'Determining the Inspection Intervals on the Predicted Cumulative Damage of Hot Components of Gas Turbines', Proc. of the 18<sup>th</sup> International Congress on Combustion Engines, Tianjin, China, 1989

[8] 'Advanced Gas Turbine (AGT) Technology Development Project', Final Report, DOE/NASA/0167-12, 1988

[9] Tsuchiya, T., Furuse, Y., Yoshino, S., Chikami, R., Tsukagoshi, K., Mori, M.: 'Development of Air-Cooled Ceramic Nozzles for a Power Generation Gas Turbine', ASME 95-GT-105, 1995

[10] Metzger, D.E., Lindstrom, G.E.: 'Impingement Cooling – A Summary and Design Recommendations', Technical Report, Airesearch Manufacturing Company of Arizona, 1970